Journal of Molecular Catalysis A: Chemical 287 (2008) 24–32

Contents lists available at ScienceDirect

Journal of Molecular Catalysis A: Chemical

journal homepage: www.elsevier.com/locate/molcata

Methyl oleate isomerization and hydrogenation over Ni/α-Al_2O_3: A kinetic study recognizing differences in the molecular size of hydrogen and organic species

María I. Cabrera [1], Ricardo J. Grau [*,1]

Instituto de Desarrollo Tecnológico para la Industria Química, INTEC, Universidad Nacional del Litoral (U.N.L.) and Consejo Nacional de Investigaciones Científicas y Técnicas (CONICET), Güemes 3450, 3000 Santa Fe, Argentina

ARTICLE INFO

Article history:
Received 2 February 2008
Received in revised form 14 February 2008
Accepted 15 February 2008
Available online 23 February 2008

Keywords:
Isomerization
Hydrogenation
Semi-competitive adsorption
Methyl oleate

ABSTRACT

The kinetics of the hydrogenation and *cis*/*trans* isomerization of methyl oleate on a Ni/α-Al_2O_3 catalyst was studied in the absence of mass-transport limitation, at 398 K ≤ T ≤ 443 K and 370 kPa ≤ P_{H_2} ≤ 650 kPa. On the basis of the Horiuti–Polanyi mechanism, involving a σ half-hydrogenated surface intermediate, a kinetic model was derived in the framework provided by the Langmuir–Hinshelwood–Hougen–Watson formalism, using the advanced concept of semi-competitive adsorption. The classical LHHW rate equations for competitive and non-competitive adsorption between the hydrogen and large organic species were matched as asymptotic cases. Statistical results clearly demonstrated the inadequacy of the model approaching non-competitive adsorption to describe the experimental data, but the residual sum of squares between experimental data and model predictions was insufficient to discriminate between the kinetic models based on competitive and semi-competitive adsorption. However, the model considering semi-competitive adsorption gave additional indication that the adsorbed molecules of *cis*- and *trans*-methyl oleate could cover up to eleven surface sites, which is in excellent agreement with a rough estimate from primary molecular modeling. This feature seems to be the most fascinating result, since it is factual and unattainable from the classical LHHW approaches. Results and distinctive features characterizing this advanced approach are highlighted. Some insights to improve parameter estimation and adsorption model discrimination are also pointed out.

1. Introduction

Since Wilhelm Normann succeeded in taking advantage of Sabatier and Senderens's method for the heterogeneous catalytic hydrogenation of organic compounds in vapor-phase and promptly performed the catalytic liquid-phase hydrogenation of unsaturated fatty acids and glycerides [1–3], the hydrogenation of vegetable oils (VOs) and fatty acid methyl esters (FAMEs) has become an important process in edible oil and oleochemical industries [4,5]. The partial hydrogenation of polyunsaturated VOs has been selectively performed for purposes of improving the flavor stability and melting properties of the final products. Its use greatly increased in the 1950s [6]. *Trans* fatty acids are products thereof and, consequently, they have been introduced into human foods but until the 1990s their adverse health implications were overlooked. Since then, the harmful effects from *trans* have been a conspicuous topic in the biomedical and health literatures [7,8]. Consequently, the market for lower non-conjugated *trans* contents in partially hydrogenated VOs has increased. Over the last two decades, there has also been increasing concern in finding non-edible uses due to the growing availability and environment compatibility of these renewable sources. Nowadays, polyunsaturated VOs used as environmentally friendly lubricants and biodiesel should be improved toward oxidation and NO_x emission by selective hydrogenation [9,10]. For these newer applications, a low content of both *trans*-isomers and saturated compounds is mandatory for preserving the fluidity of the hydrogenated products [11]. Hence, there is a renewed motivation to develop improved catalysts and, necessarily, to achieve a better understanding of the complex reaction mechanism involved in the catalytic process [12,13].

Despite the large amount of work done so far in studying the catalytic reaction kinetics, there is still need for advanced kinetic models and verification of previously reported mechanistic rate expressions, largely for *trans*-isomer formation [14]. Many kinetic studies based on the LHHW rate equations have been carried out using polyunsaturated VOs, e.g. cottonseed oil [15,16], soybean oil [17,18], sunflower seed oil [19], rapeseed oil [20], palm oil [21], and groundnut oil [22]. Triglyceride molecules having random combinations of unsaturated fatty chains, and simultaneous processes

* Corresponding author. Fax: +54 342 4511547.
E-mail address: cqfina@santafe-conicet.gov.ar (R.J. Grau).
[1] Professor at U.N.L. and Member of CONICET's Research Staff.

1381-1169/$ – see front matter © 2008 Elsevier B.V. All rights reserved.
doi:10.1016/j.molcata.2008.02.014

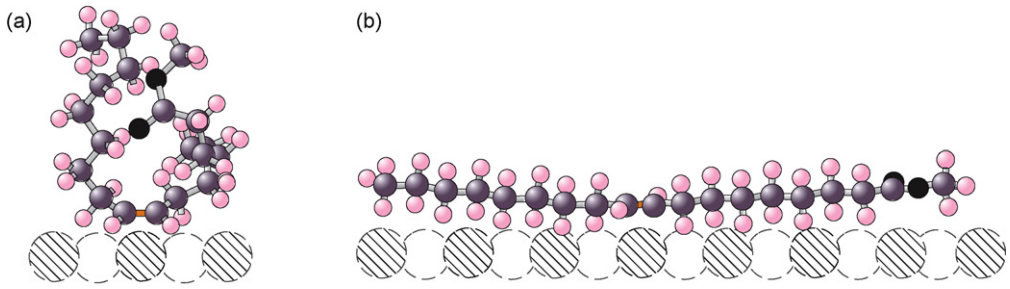

Fig. 1. Schematic representation showing: (a) *cis*-methyl oleate (**C**), and (b) *trans*-methyl oleate (**T**), both π-adsorbed on Ni(1 1 1).

of adsorption, positional and geometrical isomerization, hydrogenation, and desorption of the reacting species, sometimes in the presence of diffusion transport limitations, determine a very complex reaction system. A convenient research policy to minimize disguised kinetics and to avoid strongly statistically correlated parameters consists in uncoupling the study as described as follows [23]: first, use FAMEs as model compounds for the much more complex triglycerides that are found in VOs. Second, of course, ensure negligible mass-transport limitations. Third, analyze reaction systems of increasing complexity successively, e.g. methyl oleate, methyl linoleate, and methyl linolenate. Regarding this issue, several kinetic studies have been performed using methyl oleate [24–27], methyl linoleate [24,28–32], and methyl linolenate [24,33,34]. Only the contributions by Jonker et al. [24] and Grau et al. [26,32,34] have reported the kinetic modeling of the liquid-phase hydrogenation of each one of these three relevant FAMEs. After claiming the existence of two types of surface sites, most of these studies have been made in the framework provided by the classical LHHW non-competitive model for hydrogen (H) and VOs/FAMEs adsorption. Among other underlying assumptions, the equilibrium adsorption constants for the *cis*- and *trans*-monounsaturated FAMEs were invariably assumed to be equal, and the number of surface sites occupied by an adsorbed molecule of FAME equal to unity. The validity of these assumptions seems to be controversial from a physical viewpoint. The case of non-competitive adsorption is extreme in nature. Moreover, the mandatory distinction of two types of sites to deal with this adsorption regime would be artificial if the carbon–carbon double bonds are mainly chemisorbed as 2σ-, π- or σπ-complexes on the same type of metal surface sites as that for H adsorption. Concurrently, solving two uncoupled site balances at the surface, one for the adsorbed FAMEs and another for adsorbed H, would be somewhat ambiguous. The remaining debatable assumptions arisen from the molecular structure of *cis*- and *trans*-methyl oleate are shown in Fig. 1. It is apparent that FAME molecules occupy several surface sites. Therefore, they are not able to completely cover the catalyst surface and the competition between them is only for a fraction of the total surface sites. Moreover, the molecular structures of both geometrical isomers are quite different. The expectation of a rather flat-adsorbed molecule of *cis*-methyl oleate and a quasi-vertical adsorbed molecule of *trans*-methyl oleate is not inconceivable after viewing the optimized molecular structures. Consequently, there is no convincing reason to believe that the equilibrium adsorption constants of both isomers are equal as usually assumed. It is noteworthy that existing classical LHHW models do not properly consider steric hindrance effects of adsorbed species.

Based on the advanced concepts of multicentered adsorption [35–37] and semi-competitive adsorption [36,38–40], we recently reported the kinetic modeling of the methyl oleate hydrogenation (without *cis*/*trans* distinction) recognizing that large molecules of FAMEs could occupy several surface sites close to that (or those) interacting with the double-bond being adsorbed, and that the true adsorption regime is likely between the above mentioned extreme adsorption modes [41]. Stimulating results prompted us to examine the robustness of such approach to analyze reaction systems of increasing complexity. Accordingly, the present article is our second contribution of a series attempting to provide improved kinetic models for the liquid-phase hydrogenation of FAMEs. Herein, the intrinsic kinetics of the *cis*/*trans* isomerization and hydrogenation of methyl oleate over a Ni/α-Al_2O_3 catalyst is modeled recognizing differences in the molecular size of H and FAMEs. A semi-competitive kinetic model has been found better than those classical competitive and non-competitive ones to describe the observed kinetic behavior within the range of typical operating conditions used for industrial hydrogenation in conventional three-phase semi-batch reactors (398 K ≤ T ≤ 443 K, and 370 kPa ≤ P_{H_2} ≤ 650 kPa). Results and distinctive features characterizing this recent approach are highlighted.

2. Experimental

2.1. Catalyst and chemicals

A 25 wt.% Ni/α-Al_2O_3 catalyst (BET specific surface area 185 m^2/g, mean particle diameter 2.5 μm, mean pore diameter 8 nm) was used in all kinetic experiments. A high-vacuum distilled mixture of *cis*-methyl oleate (61.76 wt.%), *trans*-methyl oleate (26.18 wt.%) and methyl stearate (12.06 wt.%) was used in all hydrogenation experiments. Nitrogen gas (AgaGas, 99.999% pure) and hydrogen gas (AgaGas, 99.999% pure) were flowed through a Deoxo unit and a drying column before use. Methyl heptadecanoate (Aldrich, 99%) was used as internal standard in GC analyses.

2.2. Apparatus and experimental procedure

All reactions were performed in a mechanically stirred reactor (Parr Instruments Co. Model 4842). A combined system of electrical heating and coolant circulation allowed achieving a fast dynamic control of the reaction temperature, which was controlled within ±0.5 K. The pressure was measured with a strain-gauge pressure transducer (Ashcroft, Model K2) and maintained within ±5 kPa with a pressure controller (Cole Parmer, Model 68502-10). Hydrogen flow was monitored with a mass flow meter (Matheson 8110) and recorded with a data recorder (Cole Parmer, 250-mm Flatbed).

The ranges of the operating conditions were chosen to cover those typically used in industrial processing. The kinetic experiments were performed isothermally at 398, 413, 428, and 443 K, under isobaric conditions at hydrogen pressures of 370, 510, and 650 kPa. The initial catalyst loading was 0.2 wt.% with respect to the FAME mixture. The stirring rate was settled at 1000 rpm in order to guarantee the absence of mass-transfer limitations on the intrinsic reaction rate [41]. All the experiments were performed with *in situ*

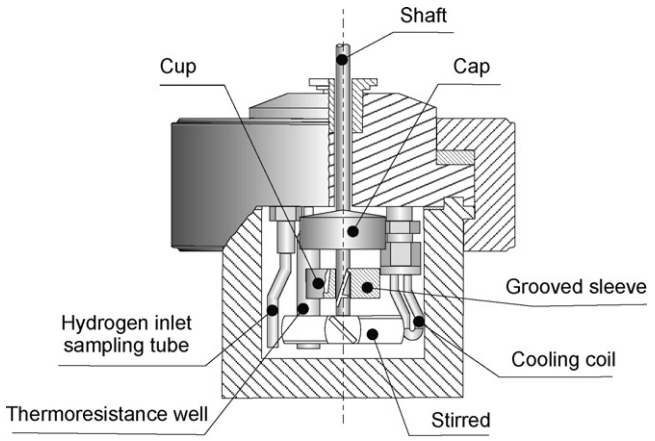

Fig. 2. Details of the hydrogenation reactor equipped with the cup-and-cap (CAC) device.

conditioning of the catalyst and reaction mixture before starting the hydrogenation reaction. A cup-and-cap (CAC) device was used for this purpose [42]. The CAC consists of a fixed cap (cover) and a mobile cup (container) sliding in a helicoidal groove machined on the stirring shaft. Two horizontal grooves allow setting the cup either at the upper part of the reaction vessel (gas-phase) or at the lowest position near the top of the impeller blades (liquid-phase), as shown in Fig. 2. The solid catalyst contained in the cup is activated under hydrogen atmosphere at the same temperature and pressure of reaction while it remains attached to the upper horizontal groove. A sudden stop of the stirring causes the fall of the cup due to the inertial effects. Then, the catalyst is fast dispersed in the hydrogen-saturated liquid-phase when the stirring rate is reinstated. Zero time was taken just at that moment because the intense turbulence instantaneously causes the dispersion of the preactivated catalyst. No induction times were observed. The reproducibility of the experimental data was ±1%. Details of the experimental setup, hydrogenation procedure and analysis of mass-transfer effects can be found in our previous contribution [41].

2.3. Analytical method

The GC analyses were performed on a gas chromatograph (Shimadzu GC-17AATF) equipped with a capillary column (SP-2330, 30 m × 0.25 mm I.D.). Nitrogen was used as carrier gas (at 0.6 mL/min). Split ratio: 100:1. The column temperature was kept constant at 463 K. The flame ionization detector (FID) and injector temperatures were 513 and 523 K, respectively. The concentrations *cis*-methyl oleate, *trans*-methyl oleate, and methyl stearate in the reaction samples were determined using methyl heptadecanoate as internal standard.

3. Kinetic model formulation

3.1. Observed kinetic behavior

Based on our experimental data, any adequate kinetic model must be able to account for the following kinetic behavior [26]:

- An overall reaction order with respect to the dissolved hydrogen concentration higher than 0.5, which increases with increasing temperature;
- A slow approaching the *cis*/*trans* equilibrium during the course of the hydrogenation, which is attained earlier at increased temperature;
- A *cis*/*trans* equilibrium ratio nearly 3.6, which is hydrogen pressure independent and slightly decreasing with increasing temperature;
- Hydrogenation rates of both geometric isomers practically equal as suggested by the nearly constant ratio of their concentrations after achieving the equilibrium at high conversion levels (methyl stearate formed >85%).

The compounds *cis*-methyl oleate (methyl oleate), *trans*-methyl oleate (methyl elaidate), and methyl stearate are hereafter referred to as **C**, **T**, and **S**, respectively. Molecular and dissociated hydrogen are denoted as $\mathbf{H}_2$ and **H**, respectively.

3.2. Reaction mechanism and underlying assumptions

A detailed reaction mechanism would have to include the simultaneous adsorption/desorption, hydrogenation, migration and geometric isomerization of double bonds. Positional isomerization would be expected to occur in some extension. It has been experimentally corroborated that the double-bond spread out fast over the hydrocarbon chain exhibiting a slight preference for the end of the chain away from the ester group as the **C** conversion increases and the double-bond mainly shifts until three positions around the Δ9 double-bond [43]. In addition, there is agreement that Δ9 and Δ10 positions appear to be the most favorable ones for the positional equilibria [43,44]. However, no distinction will be made herein on positional isomers. Even though we fully recognize that this conscious shortcoming is an oversimplification, we use it here for the sake of simplicity in highlighting main features of the methodological approach. A practical reason for this assumption is that positional isomers have little influence on the properties that are of interest for the applications mentioned in the introductory paragraph.

From a mechanistic viewpoint, the adsorbed carbon–carbon double bond can undergo either **H**-insertion or **H**-abstraction. The former would be probably easier than the latter under the adopted operating conditions, thus minimizing double-bond migration. This expectation is based on the following features. At relatively low hydrogen surface coverage, a combined **H**-abstraction/**H**-addition mechanism through π-allylic complexes would yield adsorbed species prompted to undergo double-bond migration. Conversely, at relatively high hydrogen coverage, the surface reactions likely proceed through a first **H**-addition yielding σ half-hydrogenated complexes, ready to undergo either *cis*/*trans* isomerization by free rotation of the carbon–carbon bound followed by **H**-abstraction, or a complete hydrogenation by a second **H**-addition. A positional isomerization could also occur if the above mentioned **H**-abstraction takes place from an adjacent carbon atom. Estimates from our previous kinetic model based on the recognition of the large but finite differences between the molecular sizes of the reacting species [41], revealed an **H** surface coverage ranging from 0.40 to 0.50, and an apparent fractional coverage of the methyl oleate as large as 0.42. However, the FAME fractional coverage at the catalyst surface level was less than 0.06 because a FAME molecule could cover up to seven surface sites. From the predominance of **H** chemisorbed upon the adsorbed FAMEs, **H**-addition would be probably more favorable than **H**-abstraction, thus minimizing double-bond migration under the adopted operating conditions.

Concerning the quantitative determination of the *cis*/*trans* equilibrium constant, values varying from 2 to 4 have been reported in the temperature range of 323–473 K [19,26,43,45–49]. We have determined that the equilibrium isomerization constant is practically independent of hydrogen pressure and slightly decreases with temperature ($-2.52\ \mathrm{kJ\ mol^{-1}}$), with values ranging from 3.26 to 3.57 under the present operating conditions [26]. Since these estimates

are in good agreement with available literature data [19,43,46], they will be hereafter used for the kinetic modeling. On the other hand, the literature on the **C** and **T** equilibrium adsorption constants is scarce and it has been recurrently assumed that both adsorption equilibrium constants are equal [19,24,26,27,42,50]. Analogously, the hydrogenation rates have been ordinarily considered to be equal for both isomers. As mentioned in the introductory section, there is no convincing reason to believe *a priori* that both equilibrium adsorption constants have to be equal, and this matter will be discussed below on the basis of the results from data fitting. However, although the equality of the **C** an **T** hydrogenation rates isomers is difficult to be proved because they are impossible of being determined from uncoupled processes, there is direct evidence for this assertion as concluded from the kinetic behavior observed after achieving the *cis*/*trans* equilibrium concentration ratio at high hydrogenation conversion.

Taking into account the features summarized above and other evidence on FAME hydrogenation, the rate equations are derived accepting that: (i) $\mathbf{H}_2$ dissociates upon adsorption on ⊗-sites [16,21,24–27,30,33,41]; (ii) **C** and **T** adsorb interacting with a single ⊗-site (π-adsorption) [6,13,14,41]; (iii) **S** is weakly adsorbed on the ⊗-sites; therefore, its surface coverage is assumed to be negligible in the inventory of fractional surface coverages [17,41]; (iv) adsorption/desorption rates are presumed to be fast, which implies quasi-equilibrium adsorption; (v) the adsorption equilibrium constants are not assumed to be *a priori* equal for both isomers; (vi) the fractional surface coverage by intermediate adsorbed species is negligible compared to those of bulk species [10,41–43]; (vii) no distinction is made for double-bond migration products [16,18,26,27,41]; (viii) the *cis*/*trans* isomerization and hydrogenation mechanisms are explained on the basis of the Horiuti–Polanyi mechanism involving a σ half-hydrogenated complex, as shown in Table 1 [3,10,13,17–19,33–35,39,40]; (ix) the σ-complex is in quasi-steady state; (x) the *cis*/*trans* equilibrium ratio is slowly achieved; (xi) the irreversible second **H**-addition to the σ-complex is assumed to be the rate-determining step (RDS) for the hydrogenation to deal with a reaction order greater than 0.5 and a significant simultaneous *cis*/*trans* isomerization [41,43]; (xii) the hydrogenation rate constants are assumed to be equal because the σ-complex no longer contains information concerning its previous state; (xiii) there is no activation/deactivation of ⊗-sites during the kinetic experiments performed with the preactivated catalyst; (xiv) the mass-transport rate is not limiting.

3.3. Assumptions for modeling the species competition for the adsorption on surface sites

Further basic assumptions are made for setting the elementary rate equations recognizing the differences in the molecular size of $\mathbf{H}_2$ and FAMEs (see Fig. 3) [41]: (xv) there is a unique type of ⊗-sites

Table 1
Reaction steps according to the Horiuti–Polanyi mechanism

Elementary steps		Adsorption and reaction constants
1	$\mathbf{H}_2 + 2 \otimes \rightleftarrows 2\bar{\mathbf{H}}$	$K_H = k_H/k_{-H}$
2	$\mathbf{C} + \otimes \rightleftarrows \bar{\mathbf{C}}$	$K_C = k_C/k_{-C}$
3	$\mathbf{T} + \otimes \rightleftarrows \bar{\mathbf{T}}$	$K_T = k_T/k_{-T}$
4	$\mathbf{S} + \otimes \rightleftarrows \bar{\mathbf{S}}$	$K_S = k_S/k_{-S}$
5	$\bar{\mathbf{C}} + \bar{\mathbf{H}} \rightleftarrows \sigma + \otimes$	$K_{\overline{C\sigma}} = k_{\overline{C\sigma}}/k_{-\overline{C\sigma}}$
6	$\bar{\mathbf{T}} + \bar{\mathbf{H}} \rightleftarrows \sigma + \otimes$	$K_{\overline{T\sigma}} = k_{\overline{T\sigma}}/k_{-\overline{T\sigma}}$
7	$\sigma + \bar{\mathbf{H}} \rightleftarrows \bar{\mathbf{S}} + \otimes$	k_σ

⊗ denotes surface sites for both hydrogen and FAMEs adsorption. Step 1: dissociative adsorption of $\mathbf{H}_2$. Steps 2–4: π-adsorption of FAMEs. Step 5 and 6: reversible first H-addition yielding a σ-bonded half-hydrogenated intermediate. Step 7: irreversible second H-addition affording methyl stearate.

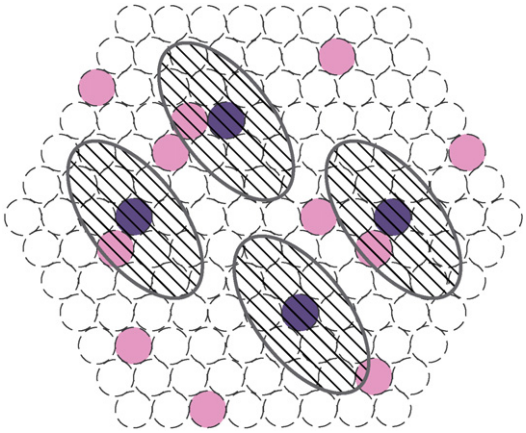

Fig. 3. Schematic top view representation of occupied-sites by adsorbed molecules of hydrogen and FAMEs (shaded regions) and covered-sites by adsorbed molecules of FAMEs (dashed regions), with uncovered-sites between them.

for the adsorption of reacting species; (xvi) there is no conjecture *a priori* on whether the $\mathbf{H}_2$ and FAMEs adsorption is competitive or non-competitive; (xvii) FAMEs molecules are much larger than both the $\mathbf{H}_2$ molecule and the distance between neighboring ⊗-sites; (xviii) a monounsaturated molecule adsorbs on one ⊗-site but additionally covers s ⊗-sites closely adjacent to that on which it is justly adsorbed; (xix) although the molecular structure is quite different for **C** and **T,** the number of additional ⊗-sites covered by a molecule is practically equal whichever the geometric isomer and, therefore, it is presumed that $s_C = s_T = s$ (see Fig. 4); (xx) the effectively covered ⊗-sites by an adsorbed molecule of **C** and **T** is $(1 + s)$, s being a parameter to be determined; (xxi) the s ⊗-sites are assumed to be inaccessible for the adsorption of another molecule of FAME due to steric hindrance, but they might be available for $\mathbf{H}_2$ adsorption; (xxii) the fractional surface coverage of free ⊗-sites is denoted as $\Theta_\otimes$ and the fraction remaining uncovered between the large molecules of FAMEs as $\Theta_\otimes^U$; (xxiii) the $\mathbf{H}_2$ adsorption rate is assumed to be proportional to $\Theta_\otimes$ while those of **C** and **T** proportional to $\Theta_\otimes^U$; (xxiv) the ratio between the occupied-sites and covered-sites by the FAMEs, so-called parameter f, does not depend on the temperature.

3.4. Elementary rate equations

Thus, the rate equation for each elementary step of the proposed mechanism can be written as

$$r_1 = k_H C_{H_2} (\Theta_\otimes)^2 - k_{-H} (\Theta_{\overline{H}})^2 \quad (1)$$

$$r_2 = k_C C_C \Theta_\otimes^U - k_{-C} \Theta_{\overline{C}} \quad (2)$$

$$r_3 = k_T C_T \Theta_\otimes^U - k_{-C} \Theta_{\overline{T}} \quad (3)$$

$$r_4 = k_S C_S \Theta_\otimes^U - k_{-S} \Theta_{\overline{S}} \quad (4)$$

$$r_5 = k_{\overline{C\sigma}} \Theta_{\overline{H}} \Theta_{\overline{C}} - k_{-\overline{C\sigma}} \Theta_\sigma \Theta_\otimes \quad (5)$$

$$r_6 = k_{\overline{T\sigma}} \Theta_{\overline{H}} \Theta_{\overline{T}} - k_{-\overline{T\sigma}} \Theta_\sigma \Theta_\otimes \quad (6)$$

$$r_7 = k_\sigma \Theta_{\overline{H}} \Theta_\sigma \quad (7)$$

where r is the reaction rate of the corresponding step per unit mass of the catalyst.

3.5. Overall rate equations

The overall consumption/generation rate equations of bulk species per unit mass of the catalyst can be described, after some algebra, by the following set of coupled equations

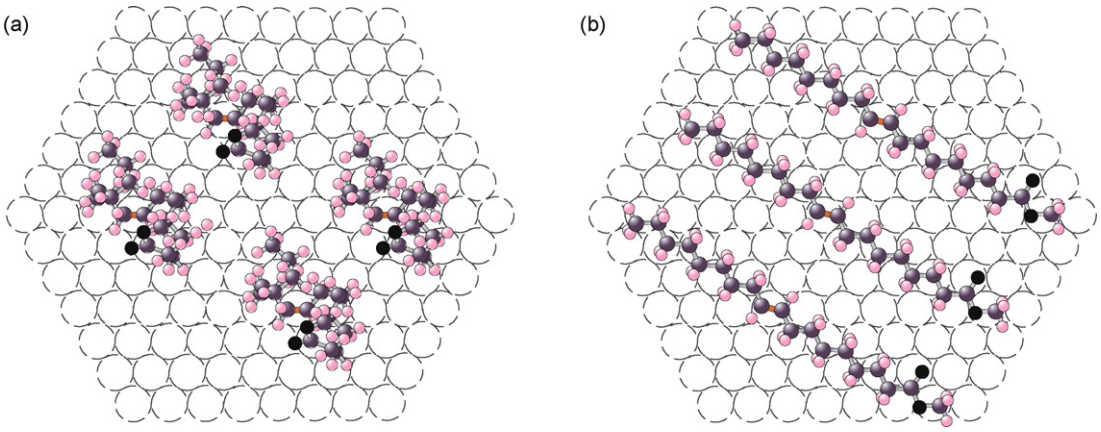

Fig. 4. Artist's view of: (a) *cis*-methyl oleate (**C**) and (b) *trans*-methyl oleate (**T**) adsorbed on Ni(1 1 1). The C9,10 double bond has been arbitrarily placed on top of Ni atoms.

$$r_C = r_6 - r_7 \tag{8}$$

$$r_T = r_5 - r_7 \tag{9}$$

$$r_S = r_7 \tag{10}$$

which fulfill the principle of mass conservation because $r_5 + r_6 - r_7 = 0$ as follows from the steady-state approximation for the σ half-hydrogenated intermediate.

Solving Eqs. (5)–(10) for second **H**-addition as RDS yields the following rate equations

$$r_C = \hat{k}_{-\overline{CT}}\sqrt{K_H C_{H_2}}\,\Theta_\otimes\Theta_{\overline{T}} - \hat{k}_{\overline{CT}}\sqrt{K_H C_{H_2}}\,\Theta_\otimes\Theta_{\overline{C}} - \hat{k}K_H C_{H_2}\Theta_\otimes\Theta_{\overline{C}} \tag{11}$$

$$r_T = -\hat{k}_{-\overline{CT}}\sqrt{K_H C_{H_2}}\,\Theta_\otimes\Theta_{\overline{T}} + \hat{k}_{\overline{CT}}\sqrt{K_H C_{H_2}}\,\Theta_\otimes\Theta_{\overline{C}} - \hat{k}K_H C_{H_2}\Theta_\otimes\Theta_{\overline{T}} \tag{12}$$

$$r_S = \hat{k}K_H C_{H_2}\Theta_\otimes[\Theta_{\overline{C}} + \Theta_{\overline{T}}] \tag{13}$$

with $\hat{k}_{\overline{CT}}$, $\hat{k}_{-\overline{CT}}$, and $\hat{k}$ being pseudo-reaction constants defined as

$$\hat{k}_{\overline{CT}} = \frac{k_{-\overline{T\sigma}}K_{\overline{C\sigma}}}{1 + k_{-\overline{T\sigma}}/k_{-\overline{C\sigma}}} \tag{14}$$

$$\hat{k}_{-\overline{CT}} = \frac{k_{-\overline{C\sigma}}K_{\overline{T\sigma}}}{1 + k_{-\overline{C\sigma}}/k_{-\overline{T\sigma}}} \tag{15}$$

$$\hat{k} = \frac{k_{\overline{\sigma}}K_{\overline{C\sigma}}}{1 + k_{-\overline{C\sigma}}/k_{-\overline{T\sigma}}} \tag{16}$$

3.6. Adsorption model

Under the quasi-equilibrium approximation for the adsorption of reactants ($r_1 = r_2 = r_3 = 0$), the fractional surface coverages can be written as

$$\Theta_{\overline{H}} = \sqrt{K_H C_{H_2}}\,\Theta_\otimes \tag{17}$$

$$\Theta_{\overline{C}} = K_C C_C \Theta_\otimes^U \tag{18}$$

$$\Theta_{\overline{T}} = K_T C_T \Theta_\otimes^U \tag{19}$$

To complete the model formulation, the adsorption model based on the concept of semi-competitive adsorption is now worked out.

3.6.1. Semi-competitive adsorption

The fractional coverages $\Theta_\otimes$ and $\Theta_\otimes^U$ must fulfill the following coupled equations

$$\Theta_{\overline{C}} + \Theta_{\overline{T}} + f(1 + \sqrt{K_H C_{H_2}})\Theta_\otimes^U = f \tag{20}$$

$$1 + f(1 + \sqrt{K_H C_{H_2}})\Theta_\otimes^U = f + (1 + \sqrt{K_H C_{H_2}})\Theta_\otimes \tag{21}$$

where

$$f = \frac{\Theta_{\overline{C}} + \Theta_{\overline{T}}}{(1 + s_C)\Theta_{\overline{C}} + (1 + s_T)\Theta_{\overline{T}}} \tag{22}$$

which can be rigorously derived from the surface site balance equation by admitting the distinction between occupied-sites and covered-sites, as demonstrated in our previous contribution [41]. It should be noted that the coverage factor f becomes a constant since it is assumed that $s_C = s_T = s$, i.e.

$$f = \frac{1}{1 + s} \tag{23}$$

where s is the number of $\otimes$-sites additionally covered by **C** and **T**, and its value remains to be estimated.

Eqs. (17)–(23) provide a workable way to survey the semi-competitive adsorption regime, which links as asymptotic cases the kinetic models for the competitive and non-competitive regimes as follows.

3.6.2. Competitive adsorption

Solving Eqs. (20) and (21) for $f = 1$ (i.e., $s = 0$) gives

$$\Theta_\otimes = \Theta_\otimes^U \tag{24}$$

$$[1 + \sqrt{K_H C_{H_2}} + K_C C_C + K_T C_T]\Theta_\otimes = 1 \tag{25}$$

which can be recognized as the classical surface site balance equation for the competitive adsorption model, with $\mathbf{H}_2$ being in dissociative form and with **C** and **T** species π-adsorbed.

3.6.3. Non-competitive adsorption

Solving Eqs. (20) and (21) for $f \to 0$ (i.e., $s > 100$) gives the following uncoupled surface site balance equations

$$[1 + \sqrt{K_H C_{H_2}}]\Theta_\otimes = 1 \tag{26}$$

$$[K_C C_C + K_T C_T]\Theta_\otimes^U = f \tag{27}$$

which are in agreement with those site balances characterizing the non-competitive adsorption model. It should be noted that Eqs. (26) and (27) were derived without having to draw the common distinction between two types of surface sites.

4. Results and discussion

4.1. Parameter estimation

Non-linear regression analysis using a modified Levenberg–Marquard algorithm combined with a procedure for solving non-linear least squares problems was performed by minimizing the

residual sum of squares (SSQ) between experimental data and model predictions [41]. The numerical integration of the hydrogenation rate equations was carried out using a Runge–Kutta (2,3) pair method. A first optimization of the kinetic parameters was achieved fitting the experimental data for all three pressures at the reference temperature of 413 K, followed by the estimation of the activation energies and adsorption heats according to the Arrhenius and Van't Hoff laws, respectively, in the 398–443 K range. The estimation of the eight unknown kinetic parameters was performed by data fitting of **T**, **C**, and **S** concentration profiles from 279 observations in both time and temperature domains. Parameter f was stepwise changed for going from competitive to non-competitive adsorption regimes, passing throughout the semi-competitive one. Estimates are within 95.5% confidence intervals. The adequacy of the fitting was checked examining the SSQ values and the residual plots.

4.2. Some insights to improve parameter estimation and adsorption model discrimination

It should be stressed that the parameter estimation is rather difficult in the framework provided by the semi-competitive model when using the resulting rate equations directly. A high correlation between parameter f and the kinetic parameters determines a small sensitivity of the objective function SSQ to f. However, it was found that some minor adaptations of both the original mathematical model and the applied numerical strategy are decidedly important to avoid this difficulty. Successful adaptations are as follows:

(1) A reduction of the number of the parameters to be estimated was made since

$$\hat{k}_{-\overline{CT}} = \frac{\hat{k}_{\overline{CT}} K_C}{K_{CT} K_T} \tag{28}$$

where the value of the *cis*/*trans* apparent equilibrium constant K_{CT} was obtained from a previous work: $K_{CT} = 3.45 \pm 0.01$ at 413 K, with $-\Delta H_{CT} = 2.52 \pm 0.15$ kJ mol^{-1} [26]. In addition, the value of equilibrium constant K_H was taken from a previous contribution: $K_H = 19.17 \pm 0.31$ at 413 K, and $-\Delta H_H = 77.70 \pm 0.73$ kJ mol^{-1} (values are for 95.5% confidence limits) [41]. Thus, the number of parameters to be estimated was reduced from 12 to 8. The unknown kinetic parameters are $\hat{k}$, $\hat{k}_{\overline{CT}}$, K_C, and K_T at 413 K, the activation energies E and E_{CT}, and the adsorption enthalpies, $-\Delta H_C$, and $-\Delta H_T$.

(2) The estimation of the activation energies and adsorption heats was performed according to the Arrhenius and Van't Hoff laws, respectively, using the well-known reparameterization

$$k(T) = k(T_0)\exp\left[\frac{-E}{RT*}\right] \tag{29}$$

$$K(T) = K(T_0)\exp\left[\frac{-\Delta H}{RT*}\right] \tag{30}$$

where T^* is given by

$$\frac{1}{T*} = \frac{1}{T} - \frac{1}{T_0} \tag{31}$$

with T_0 being the reference temperature (413 K).

(3) The parameter optimization was performed parametrically with respect to f, i.e., parameter f was stepwise varied from 0.01 to 1.00 in order to analyze the behavior of the objective function SSQ used in data fitting. Otherwise, without making the reparameterization described in the following point, optimizing f like any parameter has the risk of finding spurious conclusions about its value since it was found that SSQ could be insensitive to f values within an ample subinterval yielding SSQ minimum and, therefore, the resulting optimized value could likely result in a casual value comprised in that subinterval.

(4) A reparameterization of the adsorption constants as follows

$$\hat{K}_C = fK_C \tag{32}$$

$$\hat{K}_T = fK_T \tag{33}$$

where $\hat{K}_C$ and $\hat{K}_T$ can be understood as effective adsorption constants, allowed estimates much more insensitive to the set of initial parameters used for data fitting and less correlated estimates; consequently, a better model discrimination was possible when varying the value of parameter f. A simple inspection of the functional forms defining $\Theta_{\overline{C}}$ and $\Theta_{\overline{T}}$ reveals the encountered difficulty in the numerical solution. Indeed, from Eqs. (18)–(20) both surface coverages are given by

$$\Theta_{\overline{C}} = \frac{fK_C C_C}{K_C C_C + K_T C_T + f(1 + \sqrt{K_H C_{H_2}})} \tag{34}$$

$$\Theta_{\overline{T}} = \frac{fK_T C_T}{K_C C_C + K_T C_T + f(1 + \sqrt{K_H C_{H_2}})} \tag{35}$$

where f is in both the numerator and denominator This fact introduces difficulties in model discrimination since estimates are strongly correlated and, therefore, the resulting values of SSQ become little sensitive to varying f. On the contrary, after reparameterization according to Eqs. (32)–(35) can be rewritten as

$$\Theta_{\overline{C}} = \frac{\hat{K}_C C_C}{(1/f)(\hat{K}_C C_C + \hat{K}_T C_T) + f(1 + \sqrt{K_H C_{H_2}})} \tag{36}$$

$$\Theta_{\overline{T}} = \frac{\hat{K}_T C_T}{(1/f)(\hat{K}_C C_C + \hat{K}_T C_T) + f(1 + \sqrt{K_H C_{H_2}})} \tag{37}$$

Table 2
Estimated parameters for the competitive, semi-competitive, and non-competitive kinetic models describing the *cis*–*trans* isomerization and hydrogenation of methyl oleate, at $T = 413$ K and 370 kPa $\leq P_{H_2} \leq$ 650 kPa[a]

Parameters	Units	Adsorption model		
		Competitive	Semi-competitive	Non-competitive
f	–	1	0.09[b]	0.01
Covered ⊗-sites	–	0	11[c]	100
$\hat{k}_1 \times 10^2$	s^{-1} (g cat.)$^{-1}$	0.76 ± 0.09	3.02 ± 0.31	3.61 ± 1.02
$\hat{k}_{\overline{CT}} \times 10^2$	s^{-1} (g cat.)$^{-1}$	0.66 ± 0.05	2.84 ± 0.16	1.13 ± 0.53
$\hat{K}_C$	mol^{-1} L	69.39 ± 5.31	1.49 ± 0.08	14.22 ± 3.31
$\hat{K}_T$	mol^{-1} L	76.53 ± 6.03	1.65 ± 0.15	5.13 ± 2.43
SSQ $\times 10^6$		0.1937	0.1952	4.8230

[a] Values correspond to 95.5% confidence limits.
[b] Minimum value.
[c] Maximum value.

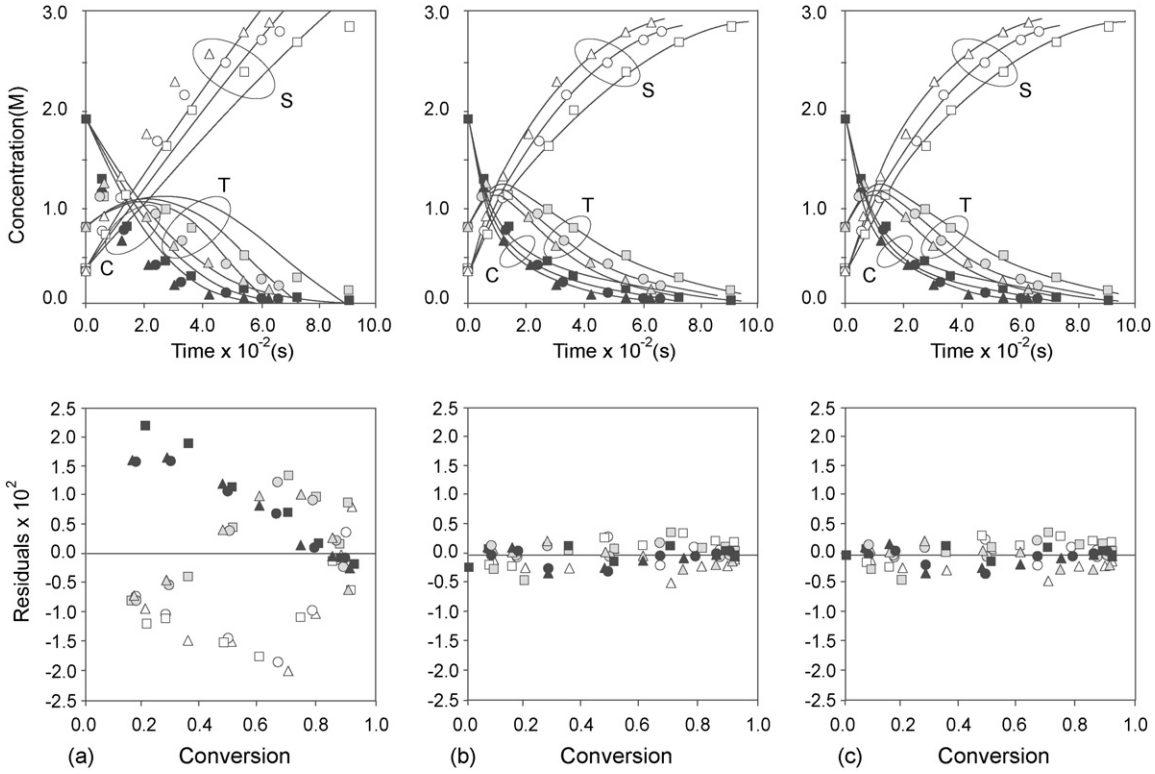

Fig. 5. Experimental and predicted composition profiles (upper figure) and residuals between predictions and experimental data (lower figure), in the time and conversion domains, respectively, at 413 K and 370 kPa (■), 510 kPa (●), and 650 kPa (▲) of hydrogen pressure. (a) Non-competitive model: $f = 0.01$. (b) Semi-competitive model: $f = 0.09$, covered-sites = 11. (c) Competitive model: $f = 1.00$, covered-sites = 1.

which are more sensitive to f than those original ones due to the fact this parameter has opposing effects on the two bracket terms in the denominator, which are associated with the competition between FAMEs and $\mathbf{H}_2$ for the surface sites. The lower the value of f, the greater is the predominance of the first term describing the FAMEs adsorption, and the lower that of the second one which is associated with the $\mathbf{H}_2$ adsorption, and viceversa. These opposing effects allowed a significant improvement in analyzing model discrimination when varying the f parameter, avoiding the risk mentioned above.

4.3. Modeling results

The results from the parameter optimization at 413 K and 370, 510, and 650 kPa, ranging f from 0.01 (non-competitive adsorption) to 1.00 (competitive adsorption) are summarized in Table 2. An inspection of the SSQ estimates reveals that a minimum constant value is obtained within the $0.09 < f < 1.00$ interval, with a steep increase of SSQ within the $0.00 < f < 0.09$ interval. This peculiarity reveals that the non-competitive model provides the worst quality of the kinetic description, while the semi-competitive and competitive models have an equivalent data-fitting capability. The corresponding experimental and predicted composition profiles as well as the residuals between the model predictions and experimental data in the conversion domain are displayed in Fig. 5. The non-uniform and broad bands of residuals certainly confirm the inadequacy of the non-competitive model (Fig. 5a), but semi-competitive and competitive models are not decidedly different from each other because they exhibit more uniform and narrow bands (Fig. 5b and c). Nevertheless, some differences between competitive and non-competitive models could be pointed out.

The kinetic constants $\hat{k}$ and $\hat{k}_{\overline{\text{CT}}}$ are higher for the semi-competitive model, whereas the equilibrium adsorption constants $\hat{K}_C$ (or K_C) and $\hat{K}_T$ (or K_T) are lower than those of the competitive model. Not unexpectedly, an unrestricted access of the **C** and **T** molecules to all the ⊗-sites, as assumed in the classical competitive model, certainly yields over-estimated equilibrium adsorption constants. As a consequence, when using this model, counterbalanced lower kinetic constant values are naturally obtained by data fitting. However, the adsorption constants K_C and K_T were found to be nearly equal, ascertaining the usual assumption. This result was certainly unexpected for us due to the expectation arising from too different molecular structures as aforementioned in the introductory paragraph. A possible reason for the equality between both equilibrium adsorption constants is that even though the blocking of access to the ⊗-sites could be greater for **T** than for **C,** the propensity of the flat-adsorbed molecule of **C** to remain adsorbed on catalytic surface could be greater than that of the quasi-vertical adsorbed molecule of **T**.

Unfortunately, with the information summarized so far it is not possible to discriminate between the competitive and semi-competitive models. An attempt to discriminate between them was made on the basis of the physical meaning of parameter f. An inspection of the plot of SSQ vs. f provides interesting advice. As can be seen from Fig. 6, within the $0.01 \leq f \leq 1$ range, the SSQ dependence with f is well-defined (i.e., clear and precise). The SSQ values do not change in the $0.09 \leq f \leq 1$ range, and they are nearly 1.95×10^{-7}, which is the minimum value of SSQ in the f domain. This means that the same data fitting quality could be obtained admitting ambiguously that a molecule of **C** or **T** could effectively cover from 1 to 11 surface sites. However, a rough estimate from primary molecular modeling suggests that a molecule of **C** or **T** on Ni(1 1 1) could cover up to 11 surface sites, as can be inferred from Fig. 4. Since these geometric restrictions can be more satisfactorily explained by the semi-competitive models than by the competitive one, the former is slightly favored. From a statistical viewpoint,

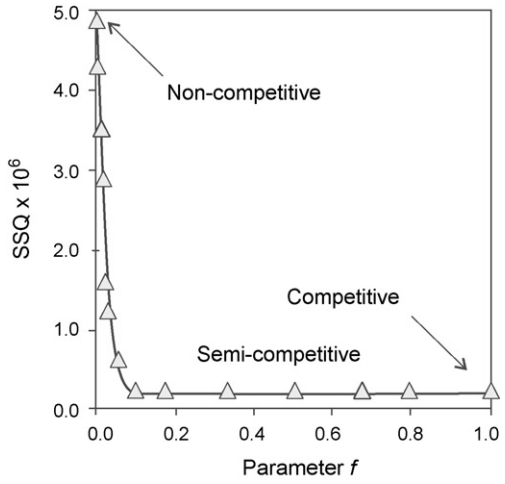

Fig. 6. Values of the residual sum of squares (*SSQ*) as a function of the occupied-sites/covered-sites ratio by a molecule of *cis*-methyl oleate (**C**) or *trans*-methyl oleate (**T**).

the semi-competitive model is also preferred as results from the correlation matrices for the estimated parameters. The obtained lower correlation between parameters of the semi-competitive model was certainly unexpected because it has been reported to be greater for this model as compared with the competitive model [40,41]. This successful result is mainly a consequence of the reparameterization expressed by Eqs. (32) and (33).

ond parameter optimization was made in the temperature domain to estimate the activation energies and adsorption heats. The results are summarized in Table 3. The estimated value for the activation energy of hydrogenation reaction E was found to be $68.49 \pm 1.23\ \mathrm{kJ\,mol^{-1}}$ Although values for E ranging from $17.7\ \mathrm{kJ\,mol^{-1}}$ [21] to $75\ \mathrm{kJ\,mol^{-1}}$ [51] have been reported in the literature, the estimated value is in excellent agreement with that of $68\ \mathrm{kJ\,mol^{-1}}$ reported in a careful kinetic study detecting mass-transport effects on double-bond migration during the methyl oleate hydrogenation using Ni on silica catalysts [52]. The estimated activation energy for the isomerization reaction of $58.09 \pm 1.87\ \mathrm{kJ\,mol^{-1}}$ is nearly 1.2 times larger than that found in a previous kinetic study based on non-competitive models [27]. A value of $33\ \mathrm{kJ\,mol^{-1}}$ has also been reported [19]. The adsorption heats for **C** and **T** were found to be -5.14 ± 0.27 and $-5.92 \pm 0.31\ \mathrm{kJ\,mol^{-1}}$, respectively. We have reported a value of nearly $-10\ \mathrm{kJ\,mol^{-1}}$ in the previous study on methyl oleate without *cis*/*trans* distinction [41]. These small values are in good agreement with other previous studies considering negligible temperature effects on the adsorption constants of unsaturated triglycerides [17,20].

5. Conclusions

Based on the pioneering concepts of multicentered adsorption and semi-competitive adsorption proposed by Salmi and Murzin's research group, and some related refinements further advanced by our research group for formulating and solving kinetic models within this framework, the kinetic modeling of the *cis*/*trans* isomerization and hydrogenation of methyl oleate on a Ni/α-Al_2O_3 catalyst in liquid-phase was successfully accomplished. The kinetic study was carried out within the range of typical operating conditions used for industrial hydrogenation in conventional three-phase semi-batch reactors ($398\ \mathrm{K} \le T \le 443\ \mathrm{K}$, and $370\ \mathrm{kPa} \le P_{H_2} \le 650\ \mathrm{kPa}$). On the basis of the Horiuti–Polanyi mechanism, a kinetic model was derived following our recent mathematical approach for deriving LHHW models based on semi-competitive adsorption. The classical LHHW rate equations for competitive and non-competitive adsorption between the hydrogen and large organic species were matched as asymptotic cases. Statistical results clearly demonstrated the inadequacy of the model approaching non-competitive adsorption to describe the experimental data, but the residual sum of squares between experimental data and model predictions was insufficient to discriminate between the kinetic models based on competitive and semi-competitive adsorption. However, the model considering semi-competitive adsorption gave additional indication that the adsorbed molecules of *cis*- and *trans*-methyl oleate could cover up to eleven surface sites, which is in excellent agreement with a rough estimate from primary molecular modeling. This feature seems to be the most fascinating result, since it is factual and unattainable from the classical LHHW approaches.

Some breakthroughs and methodological regularities have to be highlighted. Minor adaptations of both the original mathematical model and the applied numerical strategy were decidedly important to improve the parameter estimation and model

	Correlation between parameters of the competitive model (f = 1.00)				Correlation between parameters of the semi-competitive model (f = 0.09)			
	$\hat{k}$	$\hat{k}_{\overline{CT}}$	$\hat{K}_C$	$\hat{K}_T$	$\hat{k}$	$\hat{k}_{\overline{CT}}$	$\hat{K}_C$	$\hat{K}_T$
$\hat{k}$	1.000	−0.046	0.637	0.971	1.000	−0.053	0.012	0.009
$\hat{k}_{\overline{CT}}$	−0.046	1.000	0.727	−0.217	−0.053	1.000	−0.020	0.045
$\hat{K}_C$	0.637	0.727	1.000	0.466	0.012	−0.020	1.000	0.009
$\hat{K}_T$	0.971	−0.217	0.466	1.000	0.009	0.045	0.009	1.000

With the data summarized above, we decidedly inclined our preference for the semi-competitive model with $f = 0.09$. A sec-

Table 3
Fitted parameter values for the semi-competitive kinetic model describing the *cis*–*trans* isomerization and hydrogenation of methyl oleate, in the range of $398\ \mathrm{K} \le T \le 443\ \mathrm{K}$ and $370\ \mathrm{kPa} \le P_{H_2} \le 650\ \mathrm{kPa}$

Parameters	Units	Values[a]
f	–	0.09[b]
Covered ⊗-sites	–	11[c]
$\hat{k}_1 \times 10^2$	$\mathrm{s^{-1}\,(g\,cat.)^{-1}}$	3.02 ± 0.31[d]
$\hat{k}_{\overline{CT}} \times 10^2$	$\mathrm{s^{-1}\,(g\,cat.)^{-1}}$	2.84 ± 0.16[d]
$K_{C/T}$	–	3.45 ± 0.01[e]
$\hat{K}_C$	$\mathrm{mol^{-1}\,L}$	1.49 ± 0.08[d]
$\hat{K}_T$	$\mathrm{mol^{-1}\,L}$	1.65 ± 0.15[d]
K_C	$\mathrm{mol^{-1}\,L}$	16.55 ± 0.88[d]
K_T[b]	$\mathrm{mol^{-1}\,L}$	18.33 ± 1.67[d]
K_H	$\mathrm{mol^{-1}\,L}$	19.17 ± 0.31[f]
E_1	$\mathrm{kJ\,mol^{-1}}$	68.49 ± 1.23
E_{isom}	$\mathrm{kJ\,mol^{-1}}$	58.09 ± 1.87
$-\Delta H_C$	$\mathrm{kJ\,mol^{-1}}$	−5.14 ± 0.27
$-\Delta H_T$	$\mathrm{kJ\,mol^{-1}}$	−5.92 ± 0.31
$-\Delta H_H$	$\mathrm{kJ\,mol^{-1}}$	77.70 ± 0.73
$-\Delta H_{isom}$	$\mathrm{kJ\,mol^{-1}}$	2.52 ± 0.15[e]

[a] Values correspond to 95.5% confidence limits.
[b] Minimum value.
[c] Maximum value.
[d] Value at the reference temperature of 413 K.
[e] Value from the reference [26].
[f] Value from the reference [49].

discrimination using the semi-competitive model. These adaptations were the proposed reparameterizations and the analysis of the parameter optimization results in terms of f as prefixed parameter stepwise varied within the $0 < f \leq 1$ range. Furthermore, the estimated equilibrium adsorption constants were lower than those of the competitive model and the kinetic constants were higher for the semi-competitive model. Clearly, when there are large differences in the molecular size of hydrogen and organic species, the classical competitive model yields over-estimated equilibrium adsorption constants since the unrestricted access of the large molecules to all the $\otimes$-sites is a mistaken assumption. As a consequence, when using this model, counterbalanced lower kinetic constant values are naturally obtained by data fitting. We believe that the lower values of the adsorption constants and the higher values of the reaction constants predicted by the semi-competitive model are more accurate to represent the intrinsic kinetics. The additional information provided by the semi-competitive model about the probable number of surface sites covered by the organic species appears to be a fascinating result as mentioned above, but there are still too few contributions to arrive at definite conclusions. The stimulating results obtained so far would encourage further studies based on the semi-competitive model, especially on the examination of the usefulness of this advanced approach for analyzing different heterogeneous catalytic hydrogenation systems for organic synthesis.

Acknowledgments

The authors wish to express their gratitude to Agencia Nacional de Promoción Científica y Tecnológica (ANPCyT), to Consejo Nacional de Investigaciones Científicas y Técnicas (CONICET), and to Universidad Nacional del Litoral (UNL) of Argentina, for the financial support granted to this contribution.

References

[1] P. Sabatier, J.B. Senderens, C. R. Acad. Sci. Paris 124 (1897) 1358–1360.
[2] W. Normann, Verfahren zur Umwandlung ungesättigter Fettsäuren and deren Glyzeride in gesättigte Verbindungen, German Patent 139,457 (1902).
[3] W. Normann, Brit. Pat. Appl. (1903) 1515.
[4] I.V. Deliy, N.V. Maksimchuk, R. Psaro, N. Ravasio, V. Dal Santo, S. Recchia, E.A. Paukshtis, A.V. Golovin, V.A. Semikolenov, Appl. Catal. A: Gen. 279 (2005) 99–107.
[5] B. Nohair, C. Especel, G. Lafaye, P. Marécot, L.C. Hoang, J. Barbier, J. Mol. Catal. A Chem. 229 (2005) 117–126.
[6] J.W.E. Coenen, Ind. Eng. Chem. Fundam. 25 (1986) 43–52.
[7] R.P. Mensink, M.B. Katan, New Engl. J. Med. 323 (1990) 439–445.
[8] Nutritional Aspects of Cardiovascular Disease (2004) Report of the Cardiovascular Review Group of the Committee of Medical Aspects of Food Policy number 46, Department of Health 1994, HMSO.
[9] J.P. Szybist, A.L. Boehman, J.D. Taylor, R.L. McCormick, Fuel Process. Technol. 86 (2005) 1109–1126.
[10] M. Izadifar, M. Zolghadri Jahromi, J. Food Eng. 78 (2007) 1–8.
[11] N. Ravasio, F. Zaccheria, M. Gargano, S. Recchia, A. Fusi, N. Poli, R. Psaro, Appl. Catal. 233 (2002) 1–6.
[12] A.J. Wright, A. Wong, L.L. Diosady, Food Res. Intern. 36 (2003) 1069–1072.
[13] M.B. Fernández, G.M. Tonetto, G.H. Crapiste, M.L. Ferreira, D.E. Damiani, J. Mol. Catal. A Chem. 237 (2005) 67–79.
[14] J.W. Veldinsk, M.J. Bouma, N.H. Schöön, A.A.C.M. Beenackers, Catal. Rev. Sci. Eng. 39 (1997) 253–318.
[15] J. Marangozis, O.B. Keramidas, G. Paparisvas, Ind. Eng. Chem. Process Des. Dev. 16 (1977) 361–369.
[16] K. Hashimoto, K. Muroyama, S. Nagata, J. Am. Oil Chem. Soc. 48 (1971) 291–295.
[17] G. Fillion, B. Morsi, K.R. Heier, R.M. Machado, Ind. Eng. Chem. Res. 41 (2002) 697–709.
[18] A.A. Susu, A.F. Ogunye, J. Am. Oil Chem. Soc. 58 (1981) 657–661.
[19] G. Gut, J. Kosinka, A. Prabucki, A. Schuerch, Chem. Eng. Sci. 34 (1979) 1051–1056.
[20] E. Santacesaria, P. Parrella, M. Di Serio, G. Borrelli, Appl. Catal.: A Gen. 116 (1994) 269–294.
[21] A.A. Susu, A.F. Ogunke, C.O. Onyegbado, J. Appl. Chem. Biotechnol. 28 (1978) 823–833.
[22] A.A. Susu, Appl. Catal. 4 (1982) 307–320.
[23] R.J. Grau, A.E. Cassano, M.A. Baltanás, Catal. Rev. Sci. Eng. 30 (1988) 1–48.
[24] Jonker GH, Ph. D. Thesis, University of Groningen, The Netherlands (1999).
[25] J.O. Lidefelt, J. Magnusson, N.H. Schöön, J. Am. Oil Chem. Soc. 60 (1983) 603–607.
[26] R.J. Grau, A.E. Cassano, M.A. Baltanás, Ind. Chem. Eng. Process Des. Dev. 25 (1986) 722–728.
[27] G.H. Jonker, J.W. Veldsink, A.A.C.M. Beenackers, Ind. Eng. Chem. Res. 36 (1997) 1567–1579.
[28] W.A. Cordova, P. Harriot, Chem. Eng. Sci. 30 (1974) 1201–1206.
[29] K. Tsuto, P. Harriot, B. Bischoff, Ind. Eng. Chem. Fundam. 17 (1978) 199–205.
[30] J.O. Lidefelt, J. Magnusson, N.H. Schöön, J. Am. Oil. Chem. Soc. 60 (1983) 608–613.
[31] A. Yermakova, A.S. Umbetov, V.N. Bibin, React. Kinet. Catal. Lett. 27 (1985) 309–312.
[32] R.J. Grau, A.E. Cassano, M.A. Baltanás, Chem. Eng. Commun. 58 (1987) 17–36.
[33] J. Magnusson, Ind. Eng. Chem. Res. 26 (1987) 874–877.
[34] R.J. Grau, A.E. Cassano, M.A. Baltanás, Chem. Eng. Sci. 43 (1988) 1125–1132.
[35] D.Yu. Murzin, T. Salmi, S. Smeds, M. Laatikainen, M. Mustonen, E. Paatero, React. Kinet. Catal. Lett. 61 (1997) 227–236.
[36] T. Salmi, D.Yu. Murzin, J.-P. Mikkola, J. Wärna, P. Mäki-Arvela, E. Toukoniity, S. Toppinen, Ind. Eng. Chem. Res. 43 (2004) 4540–4550.
[37] D.Yu. Murzin, T. Salmi, Catalytic kinetics, 1st ed., Elsevier Sciences and Technology, USA, 2005.
[38] J.-P. Mikkola, H. Vainio, T. Salmi, R. Sjöholm, T. Ollonqvist, J. Väyrynen, Appl. Catal. 196 (2000) 143–155.
[39] E. Toukoniitty, B. Sevcikova, P. Mäki-Arvela, J. Wärna, T. Salmi, D.Yu. Murzin, J. Catal. 213 (2003) 7–16.
[40] H. Backman, A.K. Neyestanaki, D.Yu. Murzin, J. Catal. 233 (2005) 109–118.
[41] M.I. Cabrera, R.J. Grau, J. Mol. Catal. A Chem. 260 (2006) 269–279.
[42] R.J. Grau, A.E. Cassano, M.A. Baltanás, Ind. Eng. Chem. Res. 26 (1987) 18–22.
[43] M.M.P. Zieverink, M.T. Kreutzer, F. Kapteijn, J.A. Moulijn, Ind. Eng. Chem. Res. 44 (2005) 9668–9675.
[44] T. Isbell, R. Kleiman, S. Erhan, J. Am. Oil Chem. Soc. 69 (1992) 1177–1183.
[45] L.F. Albright, J. Wisniak, J. Am. Oil Chem. Soc. 39 (1962) 14–19.
[46] C. Lichfield, J.E. Lord, A.F. Isbell, R. Reiser, J. Am. Oil Chem. Soc. 40 (1963) 553–557.
[47] L.F. Albright, Chem. Eng. 11 (1967) 197–202.
[48] C. Chatgilialoglu, A. Altieri, H. Fischer, J. Am. Chem. Soc. 124 (2002) 12816–12823.
[49] S. Adhikari, H. Sprinz, O. Brede, Res. Chem. Intermediat. 27 (4–5) (2001) 549–559.
[50] G.H. Jonker, J.W. Veldsink, A.A.C.M. Beenackers, Ind. Eng. Chem. Res. 37 (1998) 4646–4656.
[51] L. Bern, M. Hell, N.H. Schöön, J. Am. Oil Chem. Soc. 52 (1975) 391–394.
[52] P. Van der Plank, J. Catal. 26 (1972) 42–50.